Proceedings of MUCEET2009
Malaysian Technical Universities Conference on Engineering and Technology
June 20-22, 2009, MS Garden Hotel, Kuantan, Pahang, Malaysia
MUCEET2009

Modeling and Engine Performance of Direct Injection Hydrogen Fueled Engine

M. M. Rahman[1], Mohammed K. Mohammed[1], Rosli A. Bakar[1], M.M. Noor[1] and K. Kadirgama[1]

Abstract- The present study explores the modeling of four cylinder direct injection hydrogen fueled engine and investigates the effect of engine speed on engine performance. GT-Power was utilized to develop the model for direct injection engine. Air-fuel ratio was varied from rich limit (AFR=27.464) to a lean limit (AFR=171.65). The rotational speed of the engine was varied from 1000 to 6000 rpm. It can be seen from the obtained results that the engine speed are greatly influence on the brake mean effective pressure (BMEP), brake specific fuel consumption (BSFC). It can be seen that the decreases of BMEP with increases of engine speed, however, increases the brake specific fuel consumption. For rich mixtures (low AFR), BMEP decreases almost linearly, then decreases it with a non-linear manner. It can be observed that the brake thermal efficiency increases nearby the richest condition and then decreases with increases of engine speed. The optimum minimum value of BSFC occurred within a range of AFR from 38.144 (ϕ = 0.9) to 49.0428 (ϕ = 0.7) for the selected range of speed. It can be seen that higher volumetric efficiency emphasizes that direct injection of hydrogen is a strong candidate solution to solve the problem of the low volumetric efficiencies of hydrogen engine. Maximum brake torque speed for hydrogen engine occurs at lower speed compared with gasoline. The present contribution suggests the direct injection fuel supply system as a strong candidate for solving the power and abnormal combustion problems.

Keywords: direct injection, hydrogen fuel, engine speed, toque, power, volumetric efficiency.

I. INTRODUCTION

Hydrogen, as alternative fuel, has unique properties give it significant advantage over other types of fuel. However, the widespread implementation of hydrogen for vehicular application is still waiting several obstacles to be solved. These obstacles are standing in the production, transpiration, storage and utilization of hydrogen. The most important one is the utilization problems [1]. Hydrogen fuel delivery system can be broken down into three main types including the carbureted injection, port fuel injection (PFI) and direct injection (DI) [2]. In direct injection, the intake valve is closed when the fuel is injected into the combustion cylinder during the compression stroke [2]. Like PFI, direct injection has long been viewed as one of the most attractive choices for supplying hydrogen fuel to combustion chamber [3]-[6]. This view is based on: its prevention for abnormal combustion: pre-ignition, backfire and knock; and the high volumetric efficiency, (since hydrogen is injected after intake valve closing). The improved volumetric efficiency and the higher heat of combustion of hydrogen compared to gasoline, provides the potential for power density to be approximately 115% that of the identical engine operated on gasoline [3]. However, it is worthy to emphasize that while direct injection solves the problem of pre-ignition in the intake manifold, it does not necessarily prevent pre-ignition within the combustion chamber [2].

In fact the difficulties and limitations accompanied with DI are more serious and severe than those of PFI. Direct injection during the compression stroke needs high pressure hydrogen and thus effectively requires liquid hydrogen storage. Metal hydrides can only provide low pressure hydrogen, compressed hydrogen could be used but this limits the effective tank contents as the tank can only be emptied down to the fuel injection pressure. Compressing gaseous hydrogen on board would mean an extra compressor and a substantial energy demand [7]. Furthermore, a high-pressure, high flow-rate hydrogen injector is required for operation at high engine speeds and to overcome the in-cylinder pressure for injection late in the compression stroke. The high pressure was defined by White et al. [3] as greater than 80 bar to ensure sonic injection velocities and high enough mass flow rates for start of injection (SOI) throughout the compression stroke.

[1]M. M. Rahman with the Automotive Excellence Center, Faculty of Mechanical Engineering, Universiti Malaysia Pahang, Tun Abdul Razak Highway, 26300 Kuantan, Malaysia (phone: +6-09-5492207, Fax: +6-09-5492244, E-mail: mustafizur@ump.edu.my).

[1]Mohammed K. Mohammed with the PhD student, Faculty of Mechanical Engineering, Universiti Malaysia Pahang, Tun Abdul Razak Highway, 26300 Kuantan, Malaysia (E mail:mohammedk_22@yahoo.com)

.[1]Rosli Abu Bakar with the Faculty of Mechanical Engineering, Universiti Malaysia Pahang, Tun Abdul Razak Highway, 26300 Kuantan, Malaysia (E-mail: rosli@ump.edu.my).

[1]M.M. Noor with the Faculty of Mechanical Engineering, Universiti Malaysia Pahang, Tun Abdul Razak Highway, 26300 Kuantan, Malaysia (E-mail: muhamad@ump.edu.my).

[1]K. Kadirgama with the Faculty of Mechanical Engineering, Universiti Malaysia Pahang, Tun Abdul Razak Highway, 26300 Kuantan, Malaysia (E-mail: kumaran@ump.edu.my).

The need for rapid mixing necessitates the use of critical flow injectors and the short time duration with late injection requires high mass flow rates. The valve leakage at the valve seat and the losses associated with the injection system are another issues [8]-[9]. Another important challenge for DI is the extremely short time for hydrogen–air mixing. For early injection (i.e., coincident with inlet valve closure (IVC)) maximum available mixing times range from approximately 20–4 ms across the speed range 1000–5000 rpm, respectively [3]. This insufficient time leads to unstable engine operation at low hydrogen-air equivalence ratios due to insufficient mixing between hydrogen and air [10]. The objectives of this study are to modeling the four-cylinder direct injection hydrogen fueled engine and investigate the effect of engine speed on performance of engine.

II. HYDROGEN ENGINE MODELING

A. Engine Performance Parameters

The brake mean effective pressure (*BMEP*) can be defined as the ratio of the brake work per cycle W_b to the cylinder volume displaced per cycle V_d, and it can be expressed as (1).

$$\mathrm{BMEP} = \frac{W_b}{V_d} \tag{1}$$

Equation (1) can be rewrite for the four stroke engine as in (2)

$$\mathrm{BMEP} = \frac{2P_b}{NV_d} \tag{2}$$

where P_b is the brake power, and N is the rotational speed.

Brake efficiency (η_b) can be defined as the ratio of the brake power P_b to the engine fuel energy as in (3):

$$\eta_b = \frac{P_b}{\dot{m}_f (LHV)} \tag{3}$$

where $\dot{m}_f$ is the fuel mass flow rate and *LHV* is the lower heating value of hydrogen.

The brake specific fuel consumption (*BSFC*) represents the fuel flow rate $\dot{m}_f$ per unit brake power output and can be expressed as in (4):

$$BSFC = \frac{\dot{m}_f}{P_b} \tag{4}$$

The volumetric efficiency (η_v) of the engine defines as the mass of air supplied through the intake valve during the intake period ($\dot{m}_a$) by comparison with a reference mass, which is that mass required to perfectly fill the swept volume under the prevailing atmospheric conditions, and can be expressed as in (5):

$$\eta_v = \frac{\dot{m}_a}{\rho_{ai} V_d} \tag{5}$$

where ρ_{ai} is the inlet air density.

B. Engine Modeling

The engine model for an in-line 4-cylinder direct injection engine was developed for this study. Engine specifications for the base engine are tabulated in table 1. The specific values of input parameters including the AFR, engine speed, and injection timing were defined in the model. The boundary condition of the intake air was defined first in the entrance of the engine. The air enters through a bell-mouth orifice to the pipe. The discharge coefficients of the bell-mouth orifice were set to 1 to ensure the smooth transition as in the real engine. The pipe of bell-mouth orifice with 0.07 m of diameter and 0.1 m of length are used in this model. The pipe connects in the intake to the air cleaner with 0.16 m of diameter and 0.25 m of length was modeled. The air cleaner pipe identical to the bell-mouth orifice connects to the manifold. A log style manifold was developed from a series of pipes and flow-splits. The intake system of the present study model is shown in figure 1. The total volume for each flow-split was 256 cm^3. The flow-splits compose from an intake and two discharges. The intake draws air from the preceding flow-split. One discharge supplies air to adjacent intake runner and the other supplies air to the next flow-split. The last discharge pipe was closed with a cup to prevent any flow through it because there is no more flow-split. The flow-splits are connected with each other via pipes with 0.09 m diameter and 0.92 m length. The junctions between the flow-splits and the intake runners were modeled with bell-mouth orifices. The discharge coefficients were also set to 1 to assure smooth transition, because in most manifolds the transition from the manifold to the runners is very smooth. The intake runners for the four cylinders were modeled as four identical pipes with .04 m diameter and 0.1 m length. Finally the intake runners were linked to the intake ports which were modeled as pipes with 0.04 m diameter and 0.08 length. The air mass flow rate in e intake port was used for hydrogen flow rate based on the imposed AFR.

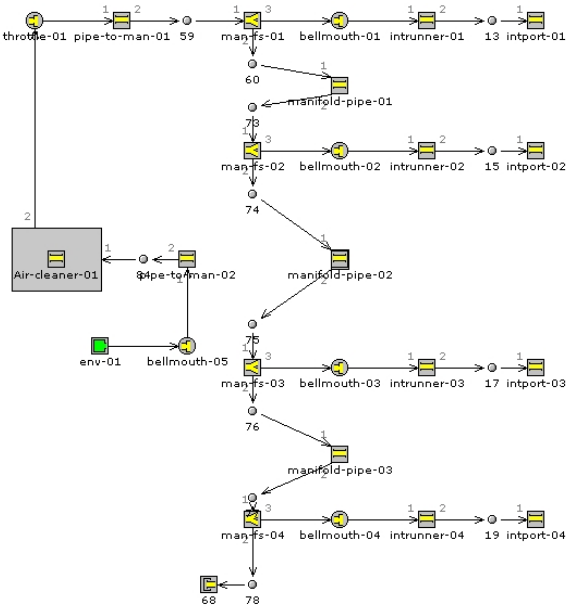

Figure 1. Intake system model.

Table1. Engine specification

Engine Parameter	Value	Unit
Bore	100	mm
Stroke	100	mm
Connecting rod length	220	mm
Piston pin offset	1.00	mm
Total displacement	3142	(cm^3)
Compression ratio	9.5	
Inlet valve close, IVC	-96	^{0}CA
Exhaust valve open, EVO	125	^{0}CA
Inlet valve open, IVO	351	^{0}CA
Exhaust valve close, EVC	398	^{0}CA

The second major part of the engine model is the powertrain model which is shown in figure 2. In the powertrain, the induced air passes through the intake cam-driven type valves with 45.5 mm of diameter to the cylinders. The valve lash (mechanical clearance between the cam lobe and the valve stem) was set to 0.1 mm. The overall temperature of the head, piston and cylinder for the engine parts are listed in table 2. The temperature of the piston is higher than the cylinder head and cylinder block wall temperature because this part is not directly cooled by the cooling liquid or oil.

Table 2. Temperature of the mail engine parts

Components	Temperature (K)
Cylinder head	550
Cylinder block wall	450
Piston	590

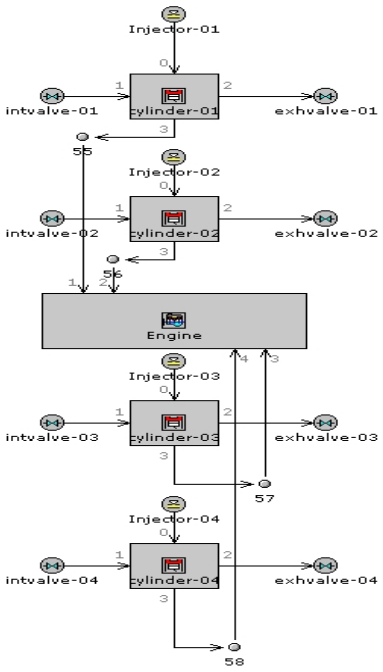

Figure 2. Powertrain model.

The last major part in the present model is the exhaust system which is shown in figure 3. The exhaust runners were modeled as rounded pipes with 0.03 m inlet diameter, and 80^0 bending angle for runners 1 and 4; and 40^0 bending angle of runners 2 and 3. Runners 1 and 4, and runners 2 and 3 are connected before enter in a flow-split with 169.646 cm^3 volume. Conservation of momentum is solved in 3-dimentional flow-splits even though the flow in GT-Power is otherwise based on a one-dimensional version of the Navier-Stokes equation. Finally a pipe with 0.06 m diameter and 0.15 m length connects the last flow-split to the environment. Exhaust system walls temperature was calculated using a model embodied in each pipe and flow-split. Table 3 are listed the parameters used in the exhaust environment of the model.

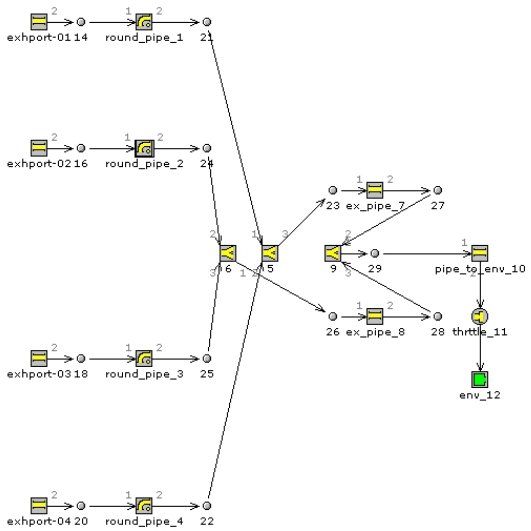

Figure 3. Exhaust system model.

Table 3. Parameters used in the exhaust environment

rsParamete	Value	Unit
External environment temperature	320	K
Heat transfer coefficient	15	W/m^2K
Radiative temperature	320	K
Wall layer material	Steel	
Layer thickness	3	mm
Emissivity	0.8	

III. RESULTS AND DISCUSSION

A lean mixture is one in which the amount of fuel is less than stoichiometric mixture. This leads to fairly easy to get an engine start. Furthermore, the combustion reaction to be more complete. Additionally, the final combustion temperature is lower reducing the amount of pollutants. It is worthy to mention that one of the most attractive combustive features for hydrogen fuel is its wide range of flammability. The air-fuel ratio AFR was varied from rich limit (AFR = 27.464:1 based on mass where the equivalence ratio (ϕ = 1.2) to a very lean limit (AFR =171.65 where ϕ = 0.2) and engine speed varied from 1000 rpm to 6000 rpm. BMEP is a good parameter for comparing engines with regard to design due to its independent on the engine size and speed.

Variation brake mean effective pressure on engine speed is shown in figure 4. It can be seen that *BMEP* decreases with increases of speed. This decrease happens with two different behaviors. For rich mixtures (low AFR), *BMEP* decreases

almost linearly, then *BMEP* falls with a non-linear behavior. Higher linear range can be recognized for higher speeds. For 4500 rpm, the linear range is continuing until AFR of 42.9125 (ϕ=0.8). The non-linear region becomes more predominant at lower speeds and the linear region cannot be specified there. The total drop of *BMEP* within the studied range of AFR was 8.08 bar for 4500 rpm compared with 10.91 bar for 2500 rpm. At lean operating conditions (AFR = 171.65, ϕ=0.2 the engine gives maximum power (*BMEP* = 1.635 bar) at lower speed 2500 rpm) compared with the power (*BMEP* = 0.24 bar) at speed 4500 rpm. Due to dissociation at high temperatures following combustion, molecular oxygen is present in the burned gases under stoichiometric conditions. Thus some additional fuel can be added and partially burned. This increases the temperature and the number of moles of the burned gases in the cylinder. These effects increases the pressure were given increase power and mean effective pressure [11].

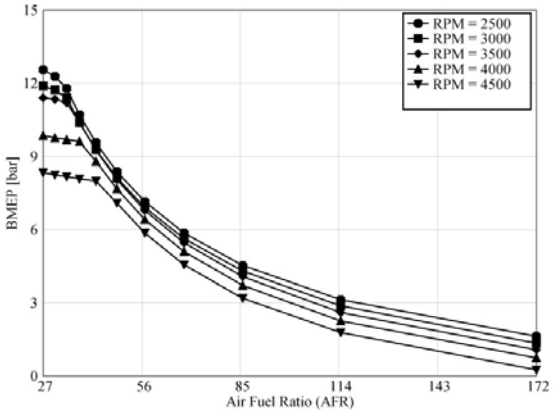

Figure 4. Variation of brake mean effective pressure with engine speed.

Figure 5 depicts the behavior of the brake specific fuel consumption *BSFC* with engine speed. It is clearly seen that the higher fuel is consumed at higher speed due to the greater friction losses that can occur at high speed. It is easy to perceive from the figure that there is an optimum minimum value of *BSFC* occurred within a range of AFR from 38.144 (ϕ=0.9) to 49.0428 (ϕ=0.7) for the selected range of speed. At very lean conditions, higher fuel consumption can be noticed. After AFR of 114.433 (ϕ=0.3) the *BSFC* rises up rapidly, especially for high speeds. At very lean conditions with AFR of 171.65 (ϕ=0.2), a *BSFC* of 125.87 *g/kW-h* was observed for the speed of 2500 rpm; while it was 809 *g/kW-h* for 4500 rpm. The value *BSFC* at speed of 2500 rpm was doubled around 2 times at speed of 4000 rpm; however the same value was doubled around 5 times at speed of 4500 rpm. This is because of very lean operation conditions can lead to unstable combustion and more lost power due to a reduction in the volumetric heating value of the air/hydrogen mixture.

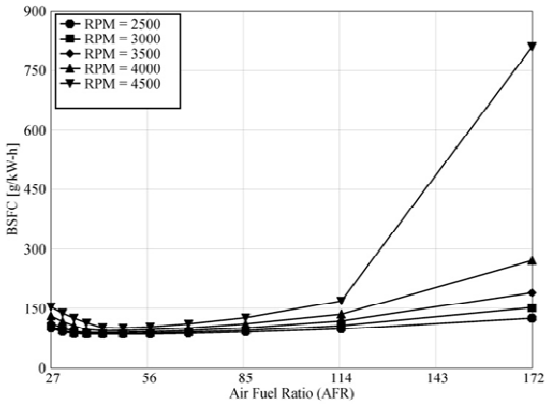

Figure 5. Variation of brake specific fuel consumption with engine speed.

Figure 6 shows the variation of the volumetric efficiency with the engine speed for different air equivalence ratio. In general, it is desirable to have maximum volumetric efficiency for engine. The importance of volumetric efficiency is more critical for hydrogen engines because of the hydrogen fuel displaces large amount of incoming air due to its low density (0.0824 kg/m^3 at 25^{0}C and 1 atm.). This reason reduces the volumetric efficiency to high extent. A stoichiometric mixture of hydrogen and air consists of approximately 30% hydrogen by volume, whereas a stoichiometric mixture of fully vaporized gasoline and air consists of approximately 2% gasoline by volume [3]. Therefore, the low volumetric efficiency for hydrogen engine is expected compared to gasoline engine works with same operating conditions and physical dimension. However, the higher volumetric efficiencies can be gained with direct injection of hydrogen, which can be shown in figure 6. Leaner mixture gives the higher volumetric efficiency. The maximum volumetric efficiency was observed 85% at lean conditions with AFR = 171.65 (ϕ =0.2) and 2500 rpm whereas volumetric efficiency decreases at high speed due to the frictional losses. In the first part of the curve, higher speed lead to higher volumetric efficiency because of the high speed gives high vacuum at the intake port and consequent larger air flow rate that goes inside the cylinder.

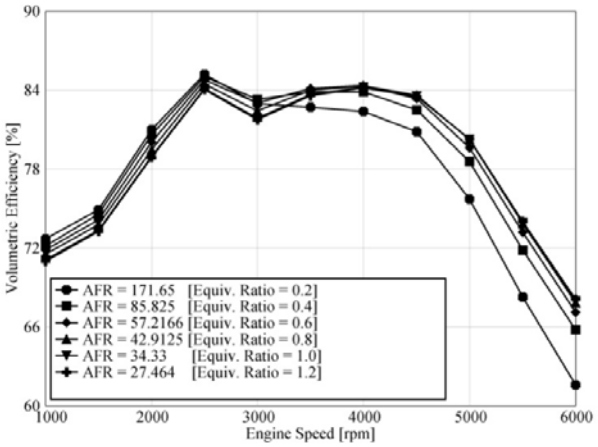

Figure 6. Effect of engine speed against volumetric efficiency for different equivalence ratio.

The maximum value of volumetric efficiency for the selected range of speed was around 85 %. At further higher engine speed beyond these values, the flow into the engine during at least part of the intake process becomes chocked. Once this condition occurs, further increases in engine speed decrease the flow rate significantly. Thus, the volumetric efficiency decreases sharply because of the higher speed is accompanied by some phenomenon that have negative influence on volumetric efficiency. These phenomenon include the charge heating in the manifold and higher friction flow losses which increase as the square of engine speed.

Figure 7 shows the variation of the power with engine speed. Greater power can be generated by increasing displacement, brake mean effective pressure and engine speed. The engine mass increases with increases of displacement and also takes up space, both are contrary to automobile design trends. For this reason, most modern engines are smaller but run at higher speeds and often turbocharged or supercharged to increase BMEP. Modern gasoline automobile engines usually have brake power output per displacement of 40 to 80 kW/L [12]. Clearly, power increases with increases of engine speed at certain level. The power decreases at higher engine speed after certain level due to the friction losses and becomes the dominant factor at very high speed. AFR has a strong effect in specifying the speed that gives maximum power. At AFR of 171.65 (ϕ =0.2), a maximum power obtained of 10.7 kW at 2500 rpm while AFR of 42.912 (ϕ=0.8), a maximum power of 94 kW obtained at 4500 rpm; and at AFR 27.464 (ϕ=1.2), a maximum power of 104.3 kW at 3500 rpm. But, for many gasoline engines, maximum power occurs at about 6000 to 7000 rpm. In fact this is another desired feature for hydrogen engines. The reported power at lean mixture is low and unacceptable.

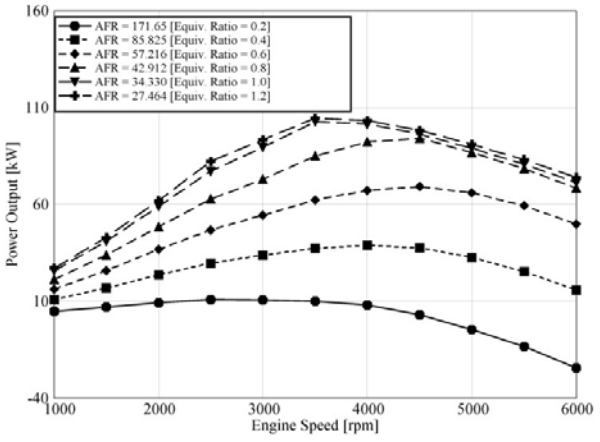

Figure 7. Effect of engine speed against power.

Figure 8 illustrates the influence of variable engine speed on the torque. Most modern gasoline automobiles have maximum torque per displacement in the range of 80 to 110 N-m/L with some as high as 140 N-m/L. The maximum torque obtained of 200 to 400 N-m, usually at engine speed around 4000 to 6000 rpm (gasoline engines) [12]. For all the range of studies AFR: at low speed, torque increases as engine speed increases. As engine speed increases further, torque reaches a maximum and then decreases as shown in figure 8. The point of maximum torque is called maximum brake torque speed (MBT). A major goal in the design of a modern automobiles engine is to flatten the torque vs. speed curve, and to have high torque at both high and low speed. But, it is important to clarify here, that toque vs. speed curve for hydrogen is flatten compared to gasoline. The BMTs for the present hydrogen engine occurred at 2500 rpm; and their values are: 178 N-m at equivalence ratio of 0.6; and 294 N-m at 2500 rpm with stoichiometric operation.

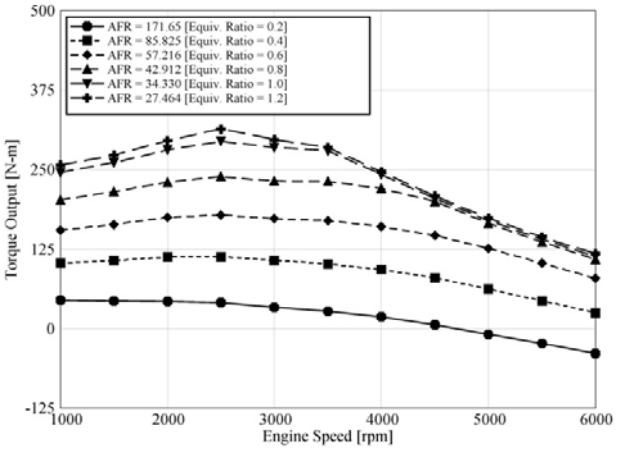

Figure 8. Variation of torque with engine speed.

IV. CONCLUSION

The following conclusions are drawn:

(i) At very lean conditions with low engine speed, acceptable *BMEP* can be reached, while it is unacceptable for higher speeds. Lean operation leads to small values of *BMEP* compared with rich conditions.

(ii) The desired minimum *BSFC* occurs within a mixture composition range of (ϕ = 0.7 to 0.9). The operation with very lean condition (ϕ<0.2) and high engine speeds (>4500) consumes unacceptable amounts of fuel.

(iii) Higher volumetric efficiency emphasizes that direct injection of hydrogen is a strong candidate solution to solve the problem of the low volumetric efficiencies of hydrogen engine.

(iv) Maximum brake torque speed for hydrogen engine occurs at lower speed compared with gasoline engines. MBT values are accepted.

ACKNOWLEDGMENT

The authors would like to thank Universiti Malaysia Pahang for provides laboratory facilities and financial support

REFERENCES

[1] N. Suwanchotchoung, "*Performance of a spark ignition dual-fueled engine using split-injection timing*". Ph.D. thesis, Vanderbilt University, Mechanical Engineering, 2003.

[2] COD (College of the Desert), "Hydrogen fuel cell engines and related technologies, module 3: Hydrogen use in internal combustion engines", Rev. 0, pp. 1-29, 2001.

[3] C.M. White, R.R. Steeper, A.E. Lutz, "The hydrogen-fueled internal combustion engine: a technical review", *Int. J. Hydrogen Energy*, 31(10):1292–1305, 2006.

[4] S. Verhelst, R. Sierens, S. Verstraeten, "A critical review of experimental research on hydrogen fueled SI engines", *Society of Automotive Engineers*, SAE paper no. 2006-01-0430, 2006.

[5] Y. Zhenzhong, W. Jianqin, F. Zhuoyi, L. Jinding, "An investigation of optimum control of ignition timing and injection system in an in-cylinder injection type hydrogen fueled engine", *Int. J. Hydrogen Energy*, vol. 27, pp. 13-217, 2002.

[6] A. Mohammadi, M. Shioji, Y. Nakai, W. Ishikura, E. Tabo, "Performance and combustion characteristics of a direct injection SI hydrogen engine", *Int. J. Hydrogen Energy*, vol. 32, pp. 296-304, 2007.

[7] S. Verhelst, "*A Study of the Combustion in Hydrogen-Fuelled Internal Combustion Engines*", Ph.D. Thesis, Department of Mechanical Engineering, Ghent University, 2005.

[8] T. Tsujimura, A. Mikami, N. Achiha, "A Study of Direct Injection Diesel Engine Fueled with Hydrogen", *Society of Automotive Engineers*, SAE paper no. 2003-01-0761, 2003.

[9] Y.Y. Kim, J.T. Lee, J.A. Caton, "The development of a dual-Injection hydrogen-fueled engine with high power and high efficiency" *Journal of Engineering for Gas Turbines and Power, ASME*, vol. 128, pp. 203-212, 2006.

[10] H. Rottengruber, M. Berckmüller, G. Elsässer, N. Brehm, C. Schwarz, "Direct-injection hydrogen SI-engine operation strategy and power density potentials", *Society of Automotive Engineers*, SAE Paper No. 2004-01-2927, 2004.

[11] C.R. Ferguson, A.T. Kirkpatrick, "*International combustion engines: Applied thermosciences*", 2nd ed., New York: John Wiley and Sons, Inc, 2001.

[12] W.W. Pulkrabek, 2003. *Engineering fundamentals of the internal combustion engines*. 2nd ed., New York: Prentic Hall, 2003.